# THERMAL RESPONSE OF CERAMIC COMPONENTS DURING ELECTRON BEAM BRAZING

**T. E. Voth, S. E. Gianoulakis, and J. A. Halbleib**
**Sandia National Laboratories**
**Albuquerque, NM**

## ABSTRACT

In this work, high-energy electron beam brazing of a ceramic part is modeled numerically. The part considered consists of a ceramic cylinder and disk between which is sandwiched an annular washer of braze material. An electron beam impinges on the disk, melting the braze metal. The resulting coupled electron-photon and thermal transport equations are solved using Monte Carlo and finite element techniques respectively. Results indicate that increased electron beam current decreases the time required to melt the braze while increasing temperature gradients in the ceramic near the braze. Furnace brazing was also simulated and predicted results indicate increased processing times relative to electron beam brazing.

## NOMENCLATURE

| | |
|---|---|
| $A$ | exposed surface area |
| $c$ | modified specific heat |
| $c^*$ | specific heat |
| $E$ | particle energy level |
| $E_k$ | electron beam kinetic energy |
| $H$ | height of alumina and braze part |
| $i$ | beam current |
| $k$ | thermal conductivity |
| $L$ | height of computational domain |
| $n$ | surface normal |
| $P$ | power |
| $q'''_{dep}$ | energy deposition rate per unit volume |
| $q''_f$ | furnace to assembly surface heat flux |
| $r$ | radial coordinate |
| $\hat{r}$ | particle location |
| $R$ | radius |
| $S$ | particle source term |
| $t$ | time |
| $T$ | temperature |
| $V$ | volume |
| $z$ | axial coordinate |

### Greek Symbols

| | |
|---|---|
| $\Delta T_{base}$ | braze to base temperature difference, $(T_b - T_{base})$ |
| $\varepsilon$ | emissivity |
| $\varphi$ | particle flux |
| $\hat{\Omega}$ | unit vector describing particle direction of travel |
| $\lambda$ | latent heat of fusion |
| $\rho$ | density |
| $\sigma$ | Stefan-Boltzmann constant |
| $\Sigma_a$ | absorption cross-section |
| $\Sigma_s$ | scattering cross-section |
| $\theta$ | dimensionless temperature, $(T - T_{in})/(T_\ell - T_{in})$ |

### Subscripts

| | |
|---|---|
| abs | absorbed |
| b | braze |
| base | base, located at $r = R_i$, $z/H = 1$ |
| beam | beam |
| c | chuck |
| cd | electron-photon transport computational domain |
| eb | electron beam |
| f | furnace |
| i | inner |
| in | initial |
| $\ell$ | liquidus |
| m | melting |
| max | maximum |
| o | outer |

| | |
|---|---|
| off | power off |
| s | solidus |
| sur | surroundings |

## INTRODUCTION

Ceramics are being used increasingly in applications where high temperatures are encountered such as automobile and gas turbine engines (Frankhouser, 1987; ASM, 1991). However, the use of ceramics is limited by a lack of methods capable of producing strong, high-temperature-resistant ceramic-to-ceramic joints. This is, in part, because many ceramic-to-ceramic joining techniques, such as brazing, require that the entire assembly be exposed to temperatures greater than their expected service temperature during processing to ensure that the braze metal melts (Schwartz, 1987). One such brazing method involves heating the part in a vacuum furnace. In a number of applications, the ceramic assembly encloses temperature sensitive components (such as electronics). Additionally, the joined materials may be damaged by high furnace temperatures (Hammond, et al., 1988). Thus, for furnace processing, low melting temperature braze materials must be used.

Alternatively, localized heating using lasers or high-energy electron beams (energies between 1 to 10 MeV) may be used to selectively heat the braze metal with neighboring components remaining relatively cool (Schwartz, 1987; Goodman et al., 1995; Turman et al., 1995). Electron beam processing has an advantage over laser processing in that the beam can be "tuned" (by adjusting beam energy) to induce volumetric heating at locations within the part which cannot be reached by a laser beam (Goodman et al., 1995). Additionally, electron beam processing is expected to be ten to twenty times cheaper than laser processing (Turman, 1992).

A disadvantage of using localized heating relative to furnace processing is that large temperature gradients produced in the part may crack the ceramic. Lower heating rates may be used to reduce gradients and minimize cracking at the expense of increased production time. Additionally, since the braze must still reach its melting temperature, lower heating rates result in increased volume-averaged part temperature, reducing the advantages of this method relative to furnace brazing.

In this work, high-energy electron beam brazing of a ceramic part is modeled numerically. Parametric simulations are performed to investigate the effect of electron beam current (and hence absorbed power) on the assembly's thermal response. To assess the advantages of electron beam brazing, the predicted thermal response of the brazed part is compared to the response for furnace processing.

## NUMERICAL MODEL

The geometry is illustrated in Figure 1. The geometry and dimensions of the assembly were designed to simulate a process under development at Sandia National Laboratories. The assembly consists of the ceramic (alumina) "part" mounted on a 7 mm thick disk of zirconium dioxide and a 6.4 mm thick aluminum chuck

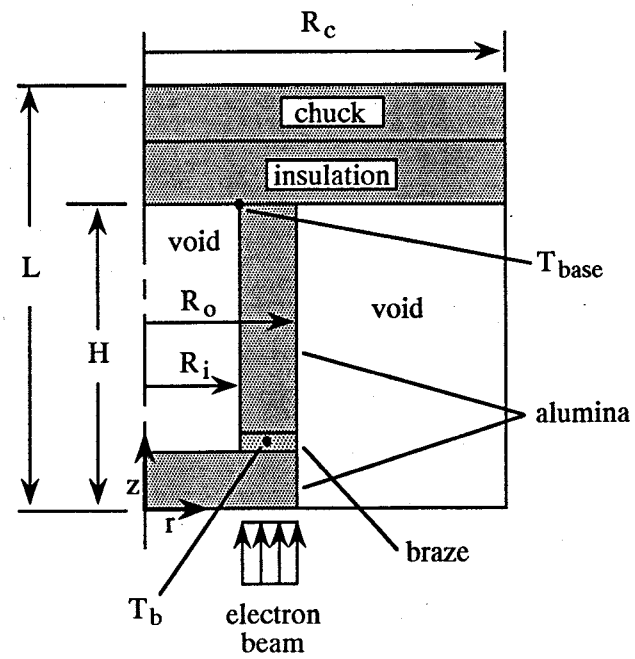


Figure 1 - Schematic of the geometry and computational domain.

both of radius $R_c$ = 50.8 mm. The zirconium dioxide serves as thermal insulation and as an absorber for stray electrons while the aluminum disk provides mechanical rigidity for the assembly. The part consists of an alumina tube ($R_i$ = 7.62 mm, $R_o$ = 12.7 mm) and a disk 5.08 mm thick between which is sandwiched a braze washer (composition 45 wt% Ag, 15 wt% Cu, 16 wt% Zn, and 24 wt% Cd) 0.2 mm thick. The part height, H, is 30.7 mm. For the analysis, the assembly and boundary conditions are assumed to be axisymmetric. Properties of the assembly materials may be found in Table 1.

The thermal response of the assembly was predicted using a one-way coupled electron-photon transport-thermal analysis. The electron-photon transport model computational domain incorporates the entire geometry as shown in Figure 1, while the thermal model computational domain is shown as the shaded region in the figure. The larger domain for the electron-photon transport problem was required to allow particle transport between assembly components which are separated by intervening voids. Coupling of the thermal and electron-photon transport response was accomplished by first predicting the temperature independent electron-photon transport within the assembly using a Monte Carlo code. The resulting energy deposition rates were then mapped onto the finite element nodes for the thermal analysis as energy generation terms. A brief description of the governing equations is provided below.

Energy deposition resulting from electron beam irradiation is simulated by coupled electron-photon transport. The transport of photons and electrons is governed by the time-independent

Table 1 - Properties used for the predictions.

| material | k (W/mK) | $c^*$ (J/kgK) | ρ (kg/m$^3$) | $T_s / T_\ell$ (K) | λ (kJ/kg) | ε |
|---|---|---|---|---|---|---|
| alumina[a] | 25.6 | 795 | 3720 | --- | --- | 0.6 |
| aluminum[b] | 237 | 903 | 2702 | --- | --- | 0.03 |
| braze[c] | 280 | 280 | 9120 | 880<br>891 | 112 | 0.3 |
| zirconium dioxide[d] | 2.1 | 628 | 5700 | --- | --- | 0.6 |

a Wesgo, 1993
b Incropera and DeWitt, 1985
c Glass, 1995d
d Touloukian, 1967

Boltzmann equation which, in conventional integro-differential form, is given by:

$$\left[\hat{\Omega}\bullet\nabla+\Sigma_s(\hat{r},E)+\Sigma_a(\hat{r},E)\right]\varphi(\hat{r},E,\hat{\Omega})= S(\hat{r},E,\hat{\Omega})+\int d\hat{\Omega}'\int dE'\,\Sigma_s(\hat{r},E'\rightarrow E,\hat{\Omega}'\rightarrow\hat{\Omega})\varphi(\hat{r},E',\hat{\Omega}') \quad (1)$$

where $\hat{\Omega}$, $\hat{r}$, and E are the particle direction of travel, location, and energy, respectively, and primed terms represent inscattered quantities. The source term is $S(r,E,\hat{\Omega})$, while $\varphi(r,E,\hat{\Omega})$ is the particle flux, and $\Sigma_a(r,E,\hat{\Omega})$ and $\Sigma_s(r,E,\hat{\Omega})$ are the absorption and scattering cross-sections respectively (Irving, 1971; Williams, 1971). The assumption of time independent transport is valid when incoming electron beam flux variations are negligible (Williams, 1971). Deterministic methods such as discrete ordinates obtain the solution via direct discretization of Eq. (1). In the Monte Carlo method used here, the Boltzmann equation is recast in integral form. Derivation and discussion of the resulting Monte Carlo form of the equations is left to the literature (Irving, 1971).

In the present application, electron-beam energy deposition was simulated with the CYLTRAN code of the Integrated TIGER Series (ITS) code system (Halbleib et al, 1992). The ITS system combines conventional microscopic (single scattering) Monte Carlo for photon transport with a macroscopic random walk for electron transport (Berger, 1963; Berger, 1988). Coupling of the two species is complete in the sense that the physical model includes all relevant processes for the production of photons by electrons and the production of electrons by photons. In addition to elastic scattering, electrons and positrons (electron antiparticles) can produce knock-on electrons, bremsstrahlung photons, annihilation radiation, and fluorescence photons and Auger electrons following electron/positron impact ionization. In addition to elastic (coherent) scattering, photons can produce electrons via incoherent scattering, electron-positron pairs via the pair-production interaction, and photoelectrons, fluorescence photons, and Auger electrons through photoelectric absorption (Halbleib et al., 1992).

The incoming electron beam was modeled as an annular source of uniform, mono-energetic, 10 MeV electrons, normally incident to the part's surface at $R_i \le r \le R_o$, $z = 0$ (see Fig. 1). The remaining boundaries are specified as non-reentrant (i.e., electrons leaving the electron-photon transport computational domain are lost). The beam was on until the braze temperature, $T_b$, at a location in the center of the braze washer (braze temperature varies spatially by less that 1 K due to its relatively high thermal conductivity, see Table 1) reaches $T_{off} = T_\ell + 25$ K. In the actual brazing process, $T_{off}$ is chosen to ensure wetting of the braze and ceramic parts (Schwartz, 1987). However, since the complex wetting dynamics are not modeled here, $T_{off}$ is chosen simply to ensure that the entire braze volume reaches $T_\ell$.

The equation governing thermal energy transport is:

$$\frac{1}{r}\frac{\partial}{\partial r}\left(kr\frac{\partial T}{\partial r}\right)+\frac{\partial}{\partial z}\left(k\frac{\partial T}{\partial z}\right)+q'''_{dep}=c\rho\frac{\partial T}{\partial t} \quad (2)$$

Braze solid-liquid phase change was modeled by varying the braze specific heat to account for the latent heat of fusion as:

$$c = c^* + \lambda/(T_s - T_\ell) \quad T_\ell \le T \le T_s$$
$$c = c^* \quad \text{otherwise} \quad (3)$$

where $T_\ell$ and $T_s$ are the liquidus and solidus temperatures respectively.

Assuming that the apparatus is enclosed in a vacuum and is radiatively insulated (with a radiation shield) only during the heating phase, the thermal boundary conditions are modeled as insulated for $t \le t_{off}$ and as:

$$\partial T/\partial n = 0 \qquad r = 0;\ 0 \le z \le L\text{: internal surfaces}$$
$$k\partial T/\partial n = \varepsilon\sigma(T^4 - T_{sur}^4)\bullet n \qquad \text{elsewhere} \quad (4)$$

for $t \ge t_{off}$ to allow cooling of the part (having removed the radiation shield). The domain is initially at $T_{in} = 298$ K while the surrounding temperature, $T_{sur} = 298$ K.

The thermal analysis was performed using COYOTE II (Gartling and Hogan, 1994). COYOTE II is a finite element code for solving the non-linear, heat diffusion equation.

Numerical experiments were performed to determine sensitivity of the results to mesh size. The number of elements, for the electron-photon transport and thermal analysis, were doubled simultaneously until $\theta_{b,max}$ changed by less than 1 percent between subsequent mesh refinements. A total of 440 Monte Carlo elements and 2200 quad elements where found to satisfy these requirements and were used for the following analysis. Finally, the Monte Carlo simulations presented here incorporated 400,000 electron histories resulting in an estimated 1-σ statistical uncertainty of approximately 1% over most of the geometry.

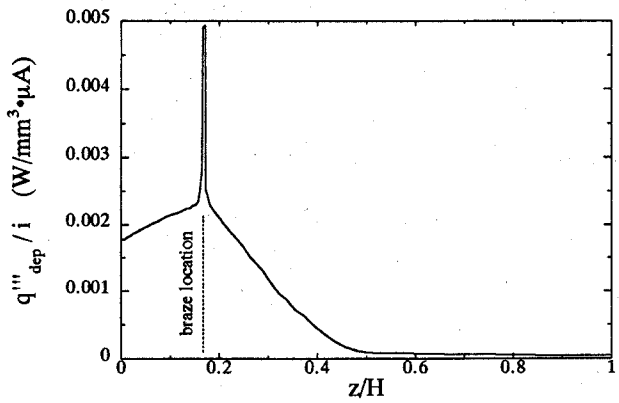


Figure 2 - Distribution of energy deposition rate per unit beam current in the part at r = 10.2 mm, $0 \leq Z/H \leq 1$. Units are in W/mm³•μA.

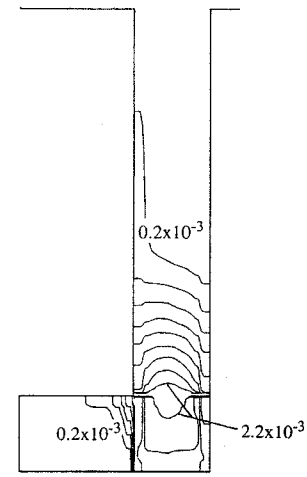


Figure 3 - Contours of energy deposition rate per unit beam current within the cylindrical section and cap. Contours are in 0.25 x $10^{-3}$ W/mm³•μA increments.

## RESULTS AND DISCUSSION

Parametric simulations for a range of beam currents, i, have been performed. Beam currents from 20 to 100 μA are investigated here as they are typical of the range of commercial beams available (Turman et al., 1995). Predicted energy deposition rate results are discussed first. Reference case thermal analysis results are then presented followed by a comparative study of the effect of beam current on the assembly's thermal response. Finally, a comparison of the thermal response of the part for both electron beam and furnace processing is made.

### Electron Beam Energy Deposition

Figure 2 shows the energy deposition rate distribution in the alumina and braze at r = 10.2 mm (halfway between $R_i$ and $R_o$). Since beam power is given as $P_{beam} = E_k \bullet i$, power absorbed by the part, $P_{abs}$, and thus $q'''_{dep}$, scale linearly with beam current. However, because not all beam energy is absorbed by the part, $P_{beam}$ and $P_{abs}$ are not equal. Note that $P_{abs}$ may be calculated by integrating $q'''_{dep}$ over the computational domain volume as

$$P_{abs} = \int_{V_{cd}} q'''_{dep}\, dV \qquad (5)$$

yielding $P_{abs} = 8.283 \bullet i$ W, where beam current has units of μA. Thus, for a beam energy of 10 MeV, $P_{abs}/P_{beam} = 0.8283$ (of course, this result is dependent on assembly geometry and materials).

Figure 2 indicates that the maximum energy deposition rate occurs in the braze material due to its higher atomic number relative to the alumina, resulting in more rapid heating of the braze. Energy deposition decreases with increased z/H for z/H > 0.17 as the electron beam energy is attenuated. Figure 3 shows the energy deposition rate contours in the alumina part. Note that the deposition contours are quite two-dimensional within the ceramic. The radial variations of $q'''_{dep}$ are attributable to i) portions of the beam which scatter out, and are reflected back into the part from the axis of symmetry (note the $0.2 \times 10^{-3}$ W/mm³ contour) and ii) more particle-material interactions in the internal regions of the ceramic relative to its sides.

### Reference Case Thermal Response

The 100 μA case was arbitrarily chosen for the reference case. Figure 4 shows the reference case thermal history for the braze temperature, $T_b$, base temperature, $T_{base}$, and braze-to-base temperature difference, $\Delta T_{base}$, as solid, short dashed and long dashed lines respectively. The $T_b$ and $T_{base}$ locations are illustrated in Fig. 1. Also shown in the Fig. 4 are the time the electron beam is turned off, $t_{off}$, and the liquidus and solidus temperatures, $T_s$ and $T_\ell$ respectively.

During the heating phase, $T_b$ increases rapidly, with $\partial T_b/\partial t$ decreasing as time progresses due to conductive losses to the cooler portions of the assembly. Once $T_b$ reaches $T_{off}$, the electron beam is turned off and the part cools radiatively. Note that during the heating phase $\partial T_{base}/\partial t$ is lower than $\partial T_b/\partial t$, resulting in $T_{base} < T_b$ throughout the history. This difference in the $T_{base}$ and $T_b$ thermal response is a result of the localized nature of electron beam heating and the effect is further illustrated by $\Delta T_{base}$. Initially, the assembly is at room temperature and $\Delta T_{base}$ is zero. After the electron beam is turned on (t > 0) $\Delta T_{base}$ begins to increase and reaches a maximum of approximately 500 K at t ≈

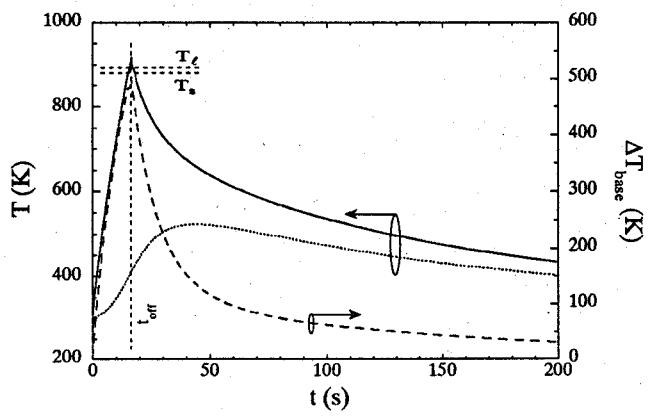


Figure 4 - Reference case (i = 100 μA) thermal response showing braze and base temperatures, and braze-to-base temperature difference histories as solid, short-dashed and long-dashed lines respectively.

$t_{off}$ = 18 s. After $t_{off}$, part temperatures equilibrate and $\Delta T_{base}$ approaches zero.

## Detailed Thermal Response for All Cases

Figure 5 (a) shows the braze and base temperature thermal histories for i = 20, 35, and 100 μA and several trends are evident. As with the reference case, at any given i, $\partial T_b/\partial t > \partial T_{base}/\partial t$. The effect of increasing beam current is to increase $\partial T_b/\partial t$ and $\partial T_{base}/\partial t$, resulting in a corresponding decrease in $T_{base,max}$ as processing times decrease. Once $T_b$ reaches $T_{off}$, the electron beam is turned off and the part cools radiatively.

Figure 5 (b) illustrates the effect of i on temperature differences across the part. As i decreases from 100 to 20 μA, $\Delta T_{base,max}$ decreases by approximately half. This reduction in $\Delta T_{base,max}$ is due to increased thermal diffusion (due to increased heating times), resulting in more uniform part temperatures relative to the reference case.

Part temperature distributions for i = 20 and 100 μA are shown in Figure 6 (a) and (b) respectively. Results are for the time when $T_b$ first reaches $T_\ell$ (t = 148.3 s and t = 16s for 20 and 100 μA cases respectively). A minimum and a maximum contour is indicated, and each intermediate contour represents a 20 K and 50 K increment for the 20 and 100 μA cases respectively. The location and value of the maximum temperature in the part is also shown. The figure again illustrates the increase in temperature gradients in the part with increased beam current. Temperature differences of approximately 250 K and 500 K from z/H = 0 to 0.8 for i = 20 and 100 μA respectively are indicated in the figure.

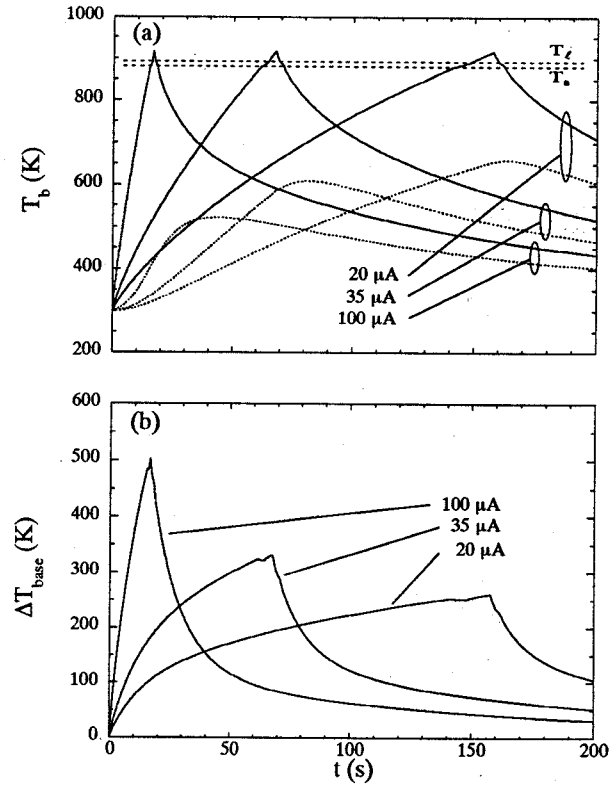


Figure 5 - Transient thermal response histories for (a) braze and base temperatures (solid and dashed lines respectively) and (b) braze-to-base temperature difference for the 20, 35, and 100 μA cases.

## Comparison to Vacuum Furnace Processing

In the previous discussion, it has been shown that electron beam processing is capable of producing very localized heating. To emphasize the advantages of electron beam processing relative to standard ceramic-to-ceramic brazing techniques a comparison is made to vacuum furnace brazing.

Furnace brazing is modeled by assuming that the entire assembly is subjected to a uniform heat flux (the heat transfer mode is not specified). Thus the thermal boundary condition due to furnace heating is

$$k\frac{\partial T}{\partial n} = q''_f \bullet n \qquad (6)$$

where $q''_f$ is the furnace supplied surface heat flux. Equation (6) is applied to all boundaries except the axis of symmetry which is assumed to be adiabatic as before. The furnace supplied heat flux, $q''_f$, is evaluated as follows

In order to make a comparison between electron beam and furnace heating, the electron beam power absorbed by the part, as evaluated using Eq. (5), is set equal to the power supplied by the

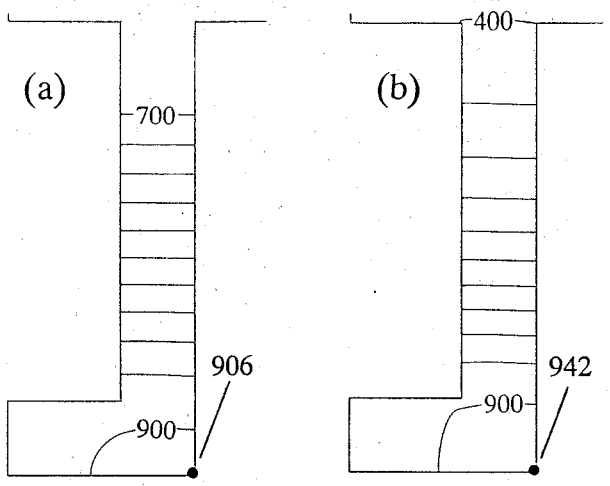


Figure 6 - Part temperature contours (in Kelvins) at $t = t_m$ for (a) the i = 20 μA and (b) the i = 100 μA cases. A minimum and a maximum contour is shown and temperature increments are 20 K and 50 K for (a) and (b) respectively. Maximum temperatures for each case are also indicated.

furnace. Utilizing Eq. (5) $P_{abs}$ = 166, 290 and 829 W for the 20, 35 and 100 μA cases respectively. The comparable furnace heat flux is calculated as $q''_f = P_{abs}/A$ where A is the assembly's exposed surface area ($1.123 \times 10^4$ mm$^2$). The resulting values for $q''_f$ are then 0.01476, 0.02583 and 0.07379 W/mm$^2$ for the 20, 35 and 100 μA cases respectively. Note that $q''_f \approx 0.07$ W/mm$^2$ for actual furnace processing (Schwartz, 1987). An additional case of i = 60 μA ($P_{abs}$ = 497 W, $q''_f$ = 0.04427 W/mm$^2$) is introduced for completion.

The thermal responses for the electron beam reference case and the corresponding vacuum furnace case ($P_{abs}$ = 829 W) are shown in Figure 7. Figure 7 (a) compares furnace and electron beam $T_b$ (solid line) as well as $T_{base}$ (dashed line) histories and shows that during the heating phase, electron beam processing induces significantly greater braze heating rates. This is because electron beam heating increases the temperature of less assembly mass relative to the furnace case. Note, also, that although the electron beam case's $\partial T_{base}/\partial t$ is greater than that for furnace processing (over most of the process history) $T_{base,max}$ for the electron beam process is less than that for furnace processing as processing time has decreased. Figure 7 (b) shows $\Delta T_{base}$, further demonstrating the localized heating produced by electron beam processing relative to furnace brazing. The electron beam $\Delta T_{base,max}$ is 3.3 times that of the furnace case. The remaining furnace and electron beam case $\Delta T_{base,max}$ values are shown as a function of absorbed power in Figure 8. It is evident from the figure that increased $P_{abs}$ results in an increase in the difference between furnace and electron beam $\Delta T_{base,max}$.

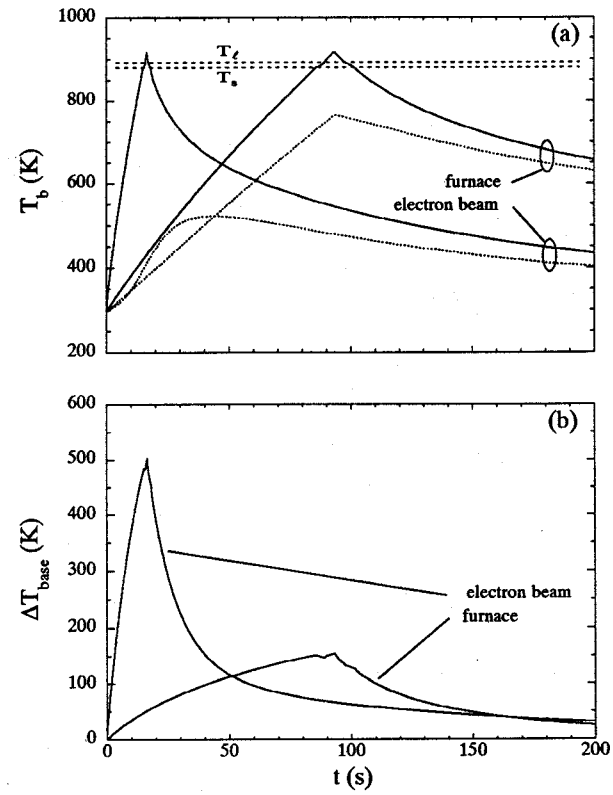


Figure 7 - Comparison of reference case electron beam and vacuum furnace transient thermal response histories for (a) braze and base temperatures (solid and dashed lines respectively) and (b) braze-to-base temperature differences.

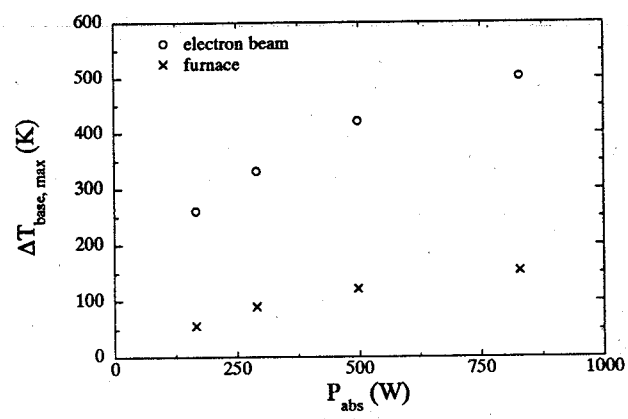


Figure 8 - Comparison of electron beam and vacuum furnace maximum braze-to-base temperature differences for a range of absorbed power.

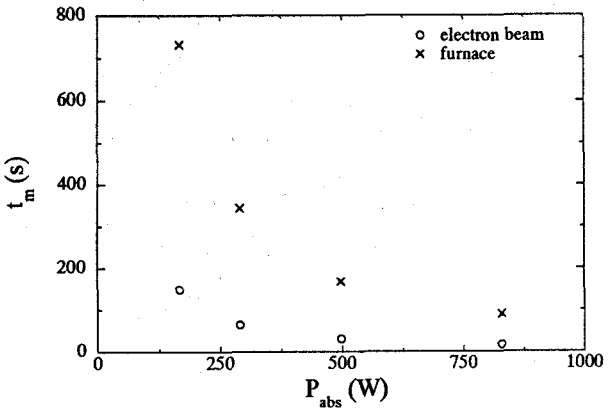


Figure 9 - Comparison of electron beam and vacuum furnace time to melt for a range of absorbed power.

Because processing time can affect final part cost, significant effort has been devoted to reducing furnace processing time (Schwartz, 1987). It is therefore of interest to compare electron beam and furnace processing times. Figure 9 (a) shows the time required for the base to reach melting, $t_m$ (assumed to be the time at which $T_b$ reaches $T_\ell$), for both electron beam and furnace processing. As $P_{abs}$ decreases, both electron beam time-to-melt, $t_{m,eb}$ and furnace time-to-melt $t_{m,f}$ increase as expected. Note that $t_{m,eb}$ and $t_{m,f}$ diverge as $P_{abs}$ decreases, with furnace heating requiring approximately 4 times longer to reach $T_\ell$ at $P_{abs}$ = 166W.

## CONCLUSIONS

A numerical model has been used to investigate the effect of beam current on the thermal response of a ceramic part during high-energy electron beam brazing. For the part considered, the results show that increasing beam current increases braze heating rate, decreasing time to melt . These increased heating rates correspond to more localized braze heating, and increased temperature differences across the part. This localized heating is advantageous from the standpoint of a cooler overall part, however, it may result in cracking problems due to high temperature gradients near the braze. For this reason, a study of the thermomechanical response of the part is recommended for future study. Finally, furnace brazing was also simulated and results show that this popular brazing method demonstrated increased melting times relative to electron beam brazing for a given power input, suggesting that processing times can be reduced with electron beam brazing.

## ACKNOWLEDGMENTS

This work was supported by the United States Department of Energy under contract DE-AC04-94ALB5000.

## REFERENCES

ASM, 1991, Engineering Materials Handbook, Ceramics and Glasses, ASM International, Metals Park, Ohio.

Berger, M. J., 1963, "Monte Carlo Calculation of the Penetration and Diffusion of Fast Charged Particles," in Methods in computational Physics, Vol. 1, Academic, New York.

Berger, M. J., 1988, "ETRAN-Experimental Benchmark" in Monte Carlo Transport of Electrons and Photons, Jenkins et al. eds., Plenum Press, New York.

Frankhouser, W. L., 1987, Advanced Processing of Ceramic Compounds, NDC, New Jersey.

Gartling, D. and Hogan, R., 1994, Coyote II - A Finite Element Computer Program for Nonlinear Heat Conduction Problems, Sandia Report Number SAND94-1179, Sandia National Laboratories, Albuquerque.

Glass, S. J., 1995, private communication, Sandia National Laboratories, Albuquerque.

Goodman, D. L., Birx, D. L. and Dave, V. R., 1995, "High Energy Electron Beam Processing Experiments with Induction Accelerators," Nuclear Instruments and Methods in Physics Research B, Vol. 99, pp. 775-779.

Halbleib, J. A., Kensek, R. P., Valdez, G. D., Seltzer, S. M. and Berger, M. J., 1992, "ITS: The Integrated TIGER Series of Electron/Photon Transport Codes - Version 3.0," IEEE Transactions of Nuclear Science, Vol. 39, pp. 1025 - 1030.

Hammond, J. P., David, S. A. and Santella, M. L., 1988, "Brazing Ceramic Oxides to Metals at Low Temperatures," Welding Journal, Vol. 67, pp. 227s-232s.

Incropera, F. P. and DeWitt, D. P., 1985, Fundamentals of Heat and Mass Transfer, 2nd ed., John Wiley & Sons, New York.

Irving, D. C., 1971, "The Adjoint Boltzmann Equation and its Simulation by Monte Carlo," Nuclear Engineering Design, Vol. 15, pp. 273-293.

Schwartz, M. M., 1987, Brazing, ASM International, Metals Park, Ohio.

Touloukian, Y. S., 1967, Thermophysical Properties of High Temperature Solid Materials, Vol. 4, The Macmillan Co., New York.

Turman, B. N., 1992, "Fundamentals of High Energy Electron Beam Generation," in Proceedings, High-Energy Electron-Beam Welding and Materials Processing Conference, ASM, Metals Park, Ohio.

Turman, B. N., Glass, S. J., Halbleib, J. A., Helmich, D. R. and Loehman, R. E., 1995, Electron Beam Joining of Structural Ceramics, Sandia Report Number SAND95-0595.

Wesgo, 1993, Technical Ceramics and Brazing Alloys Data Sheets, Wesgo Inc., Belmont, CA.

Williams, M., 1971, Mathematical Methods in Particle Transport Theory, Butterworths, London.

SF 1008-RA (FRONT 12-94)

Please replace this copy with what was sent earlier.

R

SAND No. 96-0725C Other Control N

IMPORTANT:

Is this release the result of ☐ CRADA ☐

If yes, indicate ID number _____

Has your partner reviewed and approved this relea

If no, you may not release this information without

*Onginating org. please complete sections 1 to*

**SECTION 1. Title, Author's Name, Phone, Org**

Title of report, viewgraph, video, etc. Therm Electron Beam Brazing

Principal author's name T. E. Voth

☐ Contractor to Sandia. List company name and contract no. _____ Principal Case No. 3538.040

**SECTION 2. Category of information.** Check the category that best describes your product. *Please check instructions for definitions.*

☒ Scientific and Technical information

☐ Public information to nonspecific general audiences (requires DOE pre-approval - contact Sandia Print Shop for printed material 12615 (8535), Video Services for videos 12614 (8275), or Tech Art for exhibits 12616 (8535) immediately)

DOE Distribution Category number _____ *(Required for technical reports only.)*

**SECTION 3. Format and Release Event Information.** Indicate the format(s) of the information you plan to release and provide information about the release event. See instructions.

Format: ☐ Report ☐ Publication ☐ Periodical ☐ Journal Article ☐ Abstract
☒ Conference Paper (3 copies) ☐ Slides ☐ Viewgraphs ☐ Audio/Video/Film ☐ Exhibit/Display/Poster

Release Event: Indicate name of conference, meeting or publication, the sponsoring organization, place and date of event.

Name: 1996 National Heat Transfer Conference

Organization: ASME

Place: Houston, TX Date: 8/3-5/96

**SECTION 4. Sensitive Information Review.** Indicate the classification level and category:

Title U Abstract U Total Product U

**Classification dissemination limitations:**

☐ NWD Sigma ____ ☐ CNWDI ☐ WNINTEL ☐ SUCI ☐ Other ____

☐ **Unclassified dissemination limitations** - Means this unclassified communications product contains sensitive information that requires dissemination restriction in accordance with one (or more) of the following control categories:

☐ Unclassified Controlled Nuclear Information (UCNI)
☐ Reactor Safeguards Information (RSI)
☐ Export Controlled Information (ECI)
☐ Official Use Only (OUO) exemption # _____
☐ Contains Proprietary Information (needs a Non-disclosure Agreement attached)
☐ Applied Technology
☐ Internal Distribution/Unofficial Report
☐ Small Business Innovation Research (SBIR)
☐ Protected CRADA Information
☐ Other Rationale or Program Name _____

☒ **Unrestricted dissemination** (Unlimited Release) means that distribution may be made worldwide of this unclassified information.

11B/09B

Authorized derivative classifier (ADC) T. C. Bickel (Type or print)

ADC Signature _____ ADC Org. 9113 Date 3/13/96

**SECTION 5. Intellectual Property Information.**

Has an invention disclosure (TA form) relating to the subject of this release been filed with the Sandia Patent and Licensing Office? ☐ Yes SD No. _____ ☒ No

If not, do you think an invention disclosure should be filed? ☐ Yes ☒ No

If the answer to either of the above two questions is **Yes**, when was the invention first publicly revealed (other than to Sandians or DOE personnel), if at all? Date _____

If you have any questions, please call the Sandia Patent and Licensing Office.



(Continued on page 2)

8p

**SECTION 6. Line Signatures and Approvals.** Print or type all author information; obtain appropriate signatures from next level manager and Program Manager or Center Director. Where concurrence is obtained in case of multiple authors, approval need only go through the principal author's line organization.

| Author's Names' *(print or type)* | Social Security No. | Org. No. | Phone No. | Next Level Manager's Signature | Date |
|---|---|---|---|---|---|
| Thomas E. Voth | 430-43-2332 | 9113 | 844-6004 | R.T. McGrath | 3/13/96 |
| Steven E. Giamoukis | 536-66-7252 | 9113 | 844-0450 | | |
| John Halbleib | 402-44-0043 | 9341 | 845-7064 | | |
| | | | | | |
| | | | | | |
| | | | | | |
| | | | | | |
| | | | | | |
| | | | | | |

Program Manager or Center Director (signatures depend on center policy) R.T. McGrath for 9100

**SECTION 7. Classification and Sensitive Information (13214/8535) review (MS 0175/9021).**

Signature Bruce D. Green Date 3/13/96

**SECTION 8. Patent and Licensing (11500/8535) review (MS 0161/9021).** Send to DOE/AL for contractor-authored reports.

Copyright Interest? ☐ Yes ☑ No
Patent Interest? ☐ Yes ☑ No
Patent Caution? ☐ Yes ☑ No

Signature Kermit Zy Date 3/13/96

**SECTION 9. Printing (12615/8535), Video (12614/8275), or Tech Art (12616/8535), review of public communications only (MS 0104/9021, 0551/9131, 0409/9021).**
DOE approval received _____.

Signature _____ Date _____

**SECTION 10. Technical Publications (12613/8535) review (MS 0619/9021)**

Signature Dorothy Martin Date MAR 13 1996

DOE F 1332.15
(03-93)
Combines previous version of DOE F 1332.15 and .16. All other editions are obsolete.

# U. S. DEPARTMENT OF ENERGY
# RECOMMENDATIONS FOR THE ANNOUNCEMENT AND DISTRIBUTION OF DEPARTMENT OF ENERGY (DOE) SCIENTIFIC AND TECHNICAL INFORMATION (STI)

*(See instructions on reverse side. Use plain bond paper if additional space is needed for explanations.)*

OMB Control No. 1910-1400
OMB Burden Disclosure Statement on reverse side

## PART I *(DOE, DOE Contractors, Grantees, and Awardees complete)*

### A. Product/Report Data

1. (Award) Contract No. DE-AC04-94AL85000

2. Title Thermal Response of Ceramic Components During Electron Beam Brazing

3. Product/Report Description

☐ a. Report *(Complete all that apply)*
(1) ☐ Print ☐ Nonprint *(specify)*
(2) ☐ Quarterly ☐ Semiannual ☐ Annual ☐ Final
☐ Topical ☐ Phase I ☐ Phase II
☐ Other *(specify)*
Dates covered _____ thru _____

☒ b. Conference/Meeting/Presentation *(Complete all that apply)*
(1) ☐ Print ☒ Nonprint *(specify)*
☐ Published proceedings
☐ Other *(specify)*
(2) Conference Title *(no abbreviations)* 1996 National Heat Transfer Conference
Location *(city/state/country)* Houston, TX
Date(s) *(m/d/y)* 8 /03 /96 thru *(m/d/y)* 8 /05 /96
Sponsor ASME

☐ c. Software—Additional forms are required. Follow instructions on the back of this form.

☐ d. Other *(Provide complete description)*

### B. Patent Information

| Yes | No | |
|---|---|---|
| ☐ | ☒ | Is any new equipment, process, or material disclosed? If yes, identify page numbers |
| ☐ | ☒ | Has an invention disclosure been submitted? If yes, identify the disclosure number and to whom it was submitted. Disclosure number _____ Submitted to _____ |
| ☐ | ☒ | Are there patent-related objections to the release of this STI product? If so, state the objections. |

### C. Contact *(Person knowledgeable of content)*

Name T. W. Voth
Phone (505) 844-6004
Position
Organization 9113, Sandia National Laboratories

## PART II *(DOE/DOE Contractors complete/or as instructed by DOE contracting officer)*

### A. DOE Identifiers

1. Product/Report Nos. SAND96-0725C

2. Funding Office(s) *(NOTE: Essential data)* YN010000000

### B. Copies for Transmittal to AD-21 (OSTI)

*(STI must be of sufficient quality for microfilming/copying.)*

☐ 1. One for classified processing
☐ 2. ____ *(number)* for standard classified distribution
☒ 3. Two unclassified for processing
☐ 4. ____ *(number)* for program unclassified distribution
☐ 5. UC/C Category
☐ 6. Additional instructions/explanations

*(Do not identify Sigma categories for Nuclear Weapons Data reports, and do not provide additional instructions that are inconsistent with C below.)*

### C. Recommendation *("X" at least one)*

☒ 1. Program/Standard Announcement/Distribution *(Available to U.S. and foreign public)*
☐ 2. Classified *(Standard Announcement only)*
☐ 3. Special Handling *(Legal basis must be noted below.)*
☐ a. Unclassified Controlled Nuclear Information (UCNI)
☐ b. Export Control/ITAR/EAR
☐ c. Temporary hold pending patent review
☐ d. Translations of copyrighted material
☐ e. Small Business Innovation Research (SBIR)
☐ f. Commercializable information
☐ (1) Proprietary
☐ (2) Protected CRADA information
Release date ___/___/___
☐ (3) Other *(explain)*
☐ 4. Program Directed Special Handling *(copy attached)*

### D. Releasing Official

A. Patent Clearance *("X" one)*
☐ Has been submitted for DOE patent clearance
☐ DOE patent clearance has been granted

B. Released by
*(Name)* Dorothy Martin
*(Signature)* Dorothy Martin
*(Phone)* (505) 845-8220
*(Date)* 3/18/96